Research in Astron. Astrophys. **2009** Vol. **9** No. **5**, 538 – 546
http://www.raa-journal.org *http://www.iop.org/journals/raa*

***R**esearch in*
***A**stronomy and*
***A**strophysics*

The estimations of four basic parameters for gamma-ray loud blazars *

Jun-Hui Fan[1], Yu-Hai Yuan[1], Yi Liu[1], Jing-Yi Zhang[1], Yi-Ping Qin[1], Hua Liu[1], Yong Huang[1], Jiang-He Yang[2], Hong-Guang Wang[1] and Jiang-Shui Zhang[1]

[1] Center for Astrophysics, Guangzhou University, Guangzhou 510400, China; *jhfan_cn@yahoo.com.cn*
[2] Department of Physics and Electronics Science, Hunan University of Arts and Science, Changde 415000, China

Received 2008 July 2; accepted 2008 September 2

Abstract The method used in our previous papers is adopted to estimate four basic parameters (the central black hole mass (M), the boosting factor (or Doppler factor) (δ), the propagation angle (Φ) and the distance along the axis to the site of the γ-ray production (d)) for 59 γ-ray loud blazars (20 BL Lacertae objects and 39 flat spectrum radio quasars). The central black hole masses estimated for this sample are in a range of from $10^7\,M_\odot$ to $10^9\,M_\odot$. In the case of black hole mass, there is no clear difference between BL Lacertae objects and flat spectrum radio quasars, which is consistent with the previous results suggesting that the central black hole masses do not play an important role in the evolutionary sequence of blazars.

Key words: galaxies: quasars — galaxies: BL Lacertae objects — galaxies: jet — galaxies: nuclei

1 INTRODUCTION

In a standard model of active galactic nuclei (AGNs), there is a supermassive black hole at the center, surrounded by an accretion disk. Blazars are an interesting subclass of AGNs. Blazars have two subclasses, namely BL Lacertae objects (BLs) and flat spectrum radio quasars (FSRQs). The black hole mass estimation is an interesting topic that has been studied by many authors using different methods: 1) the reverberation mapping technique (e.g., Wandel, Peterson & Malkan 1999; Kaspi et al. 2000), 2) the gas and stellar dynamics technique (see Genzel et al. 1997; Magorrian et al. 1998; Kormendy & Gebhardt 2001), 3) variability time-scale technique (Fan et al. 1999; Cheng et al. 1999; Fan 2005), 4) the broad-line width technique (Dibai 1984; Wandel & Yahil 1985; Padovani & Rafanelli 1988; Laor 1998; Mclure & Dunlop 2001; Vestergaard 2000, based on the assumption that the clouds in the broad-line region (BLR) are gravitationally bound and orbiting with Keplerian velocities). The central black hole mass is also found to be correlated with bulge luminosities (Kormendy & Richstone 1995), bulge masses (Magorrian et al. 1998), bulge velocity dispersions (Ferrarese & Merritt 2000; Gebhardt et al. 2000; Ferrarese et al. 2001), and radio power (Franceschini et al. 1998). The tight $M_{\rm BH} - \sigma$ correlation can be used, in return, to estimate the central black hole mass under the assumption that the relation holds for other sources as authors did in other papers, for example, by Barth et al. (2002) and Wu et al. (2002) who used the $M_{\rm BH} - \sigma$ relation to estimate black hole masses for Mkn 501 and other AGNs.

∗ Supported by the National Natural Science Foundation of China.

In addition, Cao (2002) estimated black hole masses for a sample of BL Lacertae objects based on the assumption that broad emission lines are emitted from clouds ionized by the radiation of the accretion disk surrounding the black hole.

It is generally believed that the escape of high energy γ-rays from the AGN depends on the $\gamma-\gamma$ pair production process because there are lots of soft photons around the central black hole. The opacity of $\gamma-\gamma$ pair production in γ-ray loud blazars can be used to constrain the basic parameters. Becker & Kafatos (1995) have calculated the γ-ray optical depth in the X-ray field of an accretion disk. They found that the γ-rays should escape preferentially along the symmetric axis of the disk, due to the strong angular dependence of the pair production cross section. The phenomenon of $\gamma-\gamma$ "focusing" is related to the more general issue of $\gamma-\gamma$ transparency, which sets a minimum distance between the central black hole and the site of γ-ray production (Bednarek 1993; Dermer & Schlickeiser 1994; Becker & Kafatos 1995; Zhang & Cheng 1997). So, the γ-rays are focused in a solid angle, $\Omega = 2\pi(1-\cos\Phi)$, suggesting the apparent observed luminosity should be expressed as $L_\gamma^{\rm obs} = \Omega D^2 F_\gamma^{\rm obs}(>100\,{\rm MeV})$, where $F_\gamma^{\rm obs}$ is the observed γ-ray energy flux, D the luminosity distance, z the redshift, and α_γ the γ-ray spectral index. The observed γ-rays from an AGN require that the jet almost points to us and that the optical depth τ is not greater than unity. The γ-rays are emitted from a solid angle, Ω, instead of being isotropic. In this sense, the non-isotropic radiation, the absorption and beaming (boosting) effects should be considered when the properties of a γ-ray loud blazar are discussed. In addition, the variability time scale perhaps brings us information about the γ-ray emission region. All those considerations supply an interesting method for estimating the central black hole mass and other basic parameters of a γ-ray loud blazar. In this paper, we found a sample with the available X-ray and γ-ray emissions and determined their parameters. In Section 2, we introduce the method and the calculation results. In Section 3, we present discussions and a brief summary. H_0 = 75 km s^{-1} Mpc^{-1} and q_0 = 0.5 are adopted throughout the paper.

2 EQUATIONS AND RESULT

2.1 Equations

In our previous papers, the method was described (Cheng et al. 1999; Fan 2005) based on the optical depth (Becker & Kafatos 1995). We derived four equations for four basic parameters, namely the central black hole mass (M), the boosting factor (or Doppler factor) (δ), the propagation angle (Φ) and the distance along the axis to the site of the γ-ray production (d) for γ-ray loud blazars.

$$\frac{d}{R_g} = 1.73\times10^3\frac{\Delta T_D}{1+z}\delta M_7^{-1},$$

$$L_{\rm iso}^{45} = \frac{\lambda 2.52\ \delta^{\alpha_\gamma+4}}{(1-\cos\Phi)(1+z)^{\alpha_\gamma-1}}M_7,$$

$$9\times\Phi^{2.5}\Big(\frac{d}{R_g}\Big)^{-\frac{2\alpha_X+3}{2}} + kM_7^{-1}\Big(\frac{d}{R_g}\Big)^{-2\alpha_X-3} = 1,$$

$$22.5\Phi^{1.5}(1-\cos\Phi) - 9\times\frac{2\alpha_X+3}{2\alpha_\gamma+8}\Phi^{2.5}\sin\Phi$$

$$-\frac{2\alpha_X+3}{\alpha_\gamma+4}kM_7^{-1}A^{-\frac{2\alpha_X+3}{2}}(1-\cos\Phi)^{-\frac{2\alpha_X+3}{2\alpha_\gamma+8}}\sin\Phi = 0, \qquad (1)$$

where k is

$$k = 4.61\times10^9\frac{\Psi(\alpha_X)(1+z)^{3+\alpha_X}F_0'(1+z-\sqrt{1+z})^2}{(2\alpha_X+1)(2\alpha_X+3)}\times$$

$$\left[\frac{\big(\frac{R_0}{R_g}\big)^{2\alpha_X+1}-\big(\frac{R_{\rm ms}}{R_g}\big)^{2\alpha_X+1}}{\big(\frac{R_{\rm ms}}{R_g}\big)^{-1}-\big(\frac{R_0}{R_g}\big)^{-1}}\right]\Big(\frac{E_\gamma}{4m_ec^2}\Big)^{\alpha_X}, \qquad (2)$$

M_7 is the black hole mass in units of $10^7\,M_\odot$, $\Psi(\alpha_X)$ a function of the X-ray spectral index, α_X, F_0' the X-ray flux parameter in units of cm^{-2} s^{-1}, m_e the electron mass, c the speed of light, $R_g = \frac{GM}{c^2}$ Schwarzschild radius, ΔT_D the time scale in units of days, λ is a parameter that links the intrinsic γ-ray luminosity and the Eddington luminosity with $L_\gamma^{\rm in} = \lambda L_{\rm Edd} = \lambda 1.26 \times 10^{45}\,M_7$, $L_{\rm iso}^{45}$ is the isotropic luminosity in units of 10^{45} erg s^{-1}, E_γ the average energy of the γ-rays, and R_0 and $R_{\rm ms}$ are, respectively, the outer and inner radii of the hot region of a two-temperature accretion disk (Becker & Kafatos 1995). Here, $R_{\rm ms} = 6\,R_g$, $R_0 = 30\,R_g$, and $E_\gamma = 1\,$GeV are adopted.

2.2 Results

We are interested in the γ-ray loud blazars with observed X-ray emissions and variable timescales. Because the variable timescales correspond to different variations in amplitude for different sources and/or different observation periods, we use the doubling timescale, $\Delta T_D = (F_{\rm min}/\Delta F)\Delta T$, as the variable timescale, where $\Delta F = F_{\rm max} - F_{\rm min}$ is the variation of the flux over time ΔT. There are few simultaneous X-ray and γ-ray band observations, so the data considered here are not simultaneous. The γ-ray data by Hartman et al. (1999) are used to calculate the γ-ray luminosity. The X-ray data from the different literatures are listed in Table 1 (Col. 1 gives the name; Col. 2: the redshift; Col. 3: identification, F stands for a flat spectral radio quasar while B for a BL Lacertae object; Col. 4: the 1 keV X-ray flux density in units of μ Jy; Col. 5: the X-ray spectral index, α_X from Fossati et al. (1998) and Donato et al. (2001). If there is no available X-ray spectral index, we used $\langle \alpha_X \rangle = 1.0$; Col. 6: references for Cols. 4 and 5; Col. 7: the flux $F(>100\,{\rm MeV})$ in units of 10^{-6} photon cm^{-2} s^{-1}, and the values are from Hartman et al. (1999); Col. 8: γ-ray spectral index; Col. 9: the doubling time scale in units of hours; Col. 10: references for Col. 9).

The intrinsic γ-ray luminosity is unknown, so we assume that it is close to the Eddington luminosity, say $\lambda L_{\rm Edd}$. In this paper, λ = 0.1 and 1.0 are adopted as we did in our previous papers (Cheng et al. 1999; Fan 2005). From the available X-ray and γ-ray data, we can estimate the central black hole mass, M_7, and three other parameters, namely the propagation angle, Φ, the boosting factor, δ, and the distance, d, which are listed in Table 2 (Col. 1: gives the names; Col. 2: the observed isotropic luminosity in units of 10^{48} erg s^{-1}; Col. 3: the central black hole mass in units of $10^7\,M_\odot$ ($\lambda = 1$); Co1. 4: the central black hole mass in units of $10^7\,M_\odot$ ($\lambda = 0.1$); Col. 5: the propagation angle ($\lambda = 1$); Col. 6: the propagation angle ($\lambda = 0.1$); Col. 7: the distance along the axis to the site of γ-ray production in units of Schwarzschild radii ($\lambda = 1$); Col. 8: the distance along the axis to the site of γ-ray production in units of Schwarzschild radii ($\lambda = 0.1$); Col. 9: the boosting factor ($\lambda = 1$); Col. 10: the boosting factor ($\lambda = 0.1$)).

Here, we only consider the sources with X-ray and γ-ray emissions. For sources with unknown variability in time scales, $\Delta T = 1$ day is adopted as Ghisellini et al. (1998) did. The relevant data are listed in Tables 1 and 2 for 59 γ-ray loud blazars.

Based on the result, the estimated mass upper limits for the whole sample are in the range of $10^7\,M_\odot$ to $10^9\,M_\odot$, namely $(0.57 \sim 60.90) \times 10^7\,M_\odot$ ($\lambda = 1.0$) or $(0.87 \sim 95) \times 10^7\,M_\odot$ ($\lambda = 0.1$). For details, see Figure 1. The real value of λ will cause uncertainty in the mass, but the uncertainty caused by λ is not large.

For the other three parameters, we found that the propagation angle, Φ, is in the range of 3.33° to 88.11° ($\lambda = 1.0$) or 3.02° to 83.31° ($\lambda = 0.1$) for the whole sample. If we consider BLs and FSRQs separately, we have $\Phi = 29.72^\circ \pm 21.96^\circ$ for BLs and $\Phi = 28.17^\circ \pm 16.23^\circ$ for FSRQs for $\lambda = 0.1$. The probability for both to come from the same distribution is 45%, see Figure 2.

The Doppler factors, δ, are in the range from 0.14 to 2.79 ($\lambda = 1.0$) or 0.18 to 3.74 ($\lambda = 0.1$) for the whole sample. If we consider BLs and FSRQs separately, we have $\delta = 0.80 \pm 0.37$ for BLs and $\delta = 1.85 \pm 0.75$ for FSRQs for $\lambda = 0.1$. The probability for both to come from the same distribution is 5.04×10^{-7}, see Figure 3.

For the γ-ray emission regions, the obtained results indicate that they are in the range of $16.02\,R_g$ to $577.54\,R_g$ ($\lambda = 1.0$) or $14.65\,R_g$ to $525.40\,R_g$ ($\lambda = 0.1$) for the whole sample. If we consider BLs and

Table 1 Origin Data for 59 γ-ray Loud Blazars

Name (1)	z (2)	ID (3)	$f_{1\mathrm{keV}}$ (4)	α_X (5)	Ref (6)	F (7)	α_γ (8)	ΔT_D (9)	Ref (10)
0202+149	1.202	F	0.06	0.68	D01	0.236	1.23	24	M78
0208–512	1.003	F	0.61	1.04	C97	9.1	0.69	134.4	D95
0219+428	0.444	B	1.56	1.6	F98	0.25	1.01	30	D95
0234+285	1.213	F	0.190		F98	0.314	1.53		
0235+164	0.940	B	2.5	1.01	M96	0.65	1.85	72	M96
0336–019	0.852	F	0.253		F98	1.78	0.84	2.4	W71
0420–014	0.915	F	1.08	0.67	F98	0.64	1.44	33.6	D95
0440–003	0.844	F	0.109		F98	0.86	1.37	2.64	W71
B0454–234	1.009	F	0.055		D01	0.147	2.14		
0454–463	0.858	F	0.160		F98	0.228	1.75		
B0458–020	2.286	F	0.1	0.67	D95	0.68	1.45	144	D95
0506–612	1.093	F	0.280		D01	0.288	1.40		
B0521–365	0.055	B	1.78	0.68	D95	0.32	1.63	72	D95
0528+134	2.060	F	0.65	0.54	C97	3.08	1.21	24	D95
B0537–286	3.104	F	0.18	1.36	D01	0.190	1.47		
0537–441	0.894	F	0.81	1.16	C97	2.00	1	16	H96
0716+714	0.300	B	1.35	1.77	F98	0.46	1.19	1.92	D95
0735+178	0.424	B	0.248	1.34	F98	0.3	1.60	28.8	D95
0804+499	1.433	F	0.17	1.56	D01	0.15	1.15		
0827+243	0.939	F	0.34		F98	0.7	1.42	1.32	X04
0829+046	0.180	B	1.07	0.67	D95	0.34	1.47	24	D95
0836+710	2.172	F	0.819	0.42	F98	0.33	1.62	24	D95
0851+202	0.306	B	1.063	1.5	F98	0.158	1.03	1.08	X02
0906+430	0.670	F	0.110	1.57	F98	0.32	1.35		
0917+449	2.180	F	0.47	1.39	D01	0.33	1.19		
0954+556	0.909	F	0.1	2.17	F98	0.47	1.12		
0954+658	0.368	B	0.16	1.96	F98	0.2	1.08	48	X02
1011+496	0.2	B	2.35	1.49	F98	0.13	0.90		
1055+567	0.410	B	0.47	2.31	D01	0.16	1.51		
1101+384	0.031	B	37.33	2.1	F98	0.27	0.57	1.92	D95
B1127–145	1.187	F	0.659	3.06	F98	0.35	1.70	6	W71
1156+295	0.729	F	0.44	2.3	D01	0.63	0.98	11.04	D95
1219+285	0.102	B	0.409	0.89	F98	0.54	0.73	3.58	X91
1222+216	0.435	F	0.41		D01	0.48	1.28		
1226+023	0.158	F	12.07	0.81	F98	0.09	1.58	24	D95
B1229–021	1.045	F	0.08		D01	0.16	1.85		
1253–055	0.537	F	2.43	0.68	H96	2.8	1.02	12	K93
1253–055	0.538	F	2	0.78	L98	11	0.97	6	W98
1331+170	2.084	F	0.053		D01	0.33	1.41		
B1334–127	0.539	B	0.45	1.63	D01	0.2	1.62		
B1510–089	0.361	F	0.718	0.9	F98	0.49	1.47	57.6	D95
1604+159	0.357	B	0.17		D01	0.4	1.06		
1606+106	1.227	F	0.08		F98	0.62	1.63		
1611+343	1.404	F	0.24	1.76	F98	0.69	1.42		
1622-297	0.815	F	0.08	0.67	M97	17	0.87	4.85	M97
1633+382	1.814	F	0.42	0.53	C97	0.96	0.86	16	M93
1652+398	0.033	B	10.1	1.6	C97	0.32	0.68	6	Q96
1730–130	0.902	B	0.63		D01	1.05	1.23		
1739+522	1.375	F	0.16		D01	0.41	1.42		
B1741–038	1.054	F	2.213		F98	0.49	1.42		
1830–210	1.000	F	0.43		D01	0.99	1.59		
1933–400	0.966	F	0.38		D01	0.94	1.86		
2005–489	0.071	B	25.38	2.32	F98	0.2	1.2		
2032+107	0.601	B	1.22		D01	0.36	1.83		
2052–474	1.489	F	0.28		F98	0.26	1.04		
B2155–304	0.117	B	0.058	1.25	U97	0.34	0.56	3.3	Ch99
2200+420	0.070	B	1.84	1.31	P96	1.71	0.68	3.2	B97
2230+114	1.040	F	0.486	0.67	F98	0.51	1.45	48	P88
2251+158	0.859	F	1.08	0.62	F98	1.16	1.21	1.92	D95
2356+196	1.066	F	0.28		D01	0.26	1.09		

Table 2 Four Basic Parameters for 59 γ-ray Loud Blazars

Name	$L_{\rm iso}^{48}$	M_1	$M_{0.1}$	ϕ_1	$\phi_{0.1}$	$\frac{d}{R_g}_1$	$\frac{d}{R_g}_{0.1}$	δ_1	$\delta_{0.1}$
(1)	(2)	(3)	(4)	(5)	(6)	(7)	(8)	(9)	(10)
0202+149	0.1295	8.04	11.66	14.95	13.87	89.33	82.00	0.91	1.22
0208–512	2.0000	60.90	95.00	22.39	20.69	65.32	60.50	1.17	1.59
0219+428	0.0180	19.73	29.80	40.53	37.89	48.34	45.68	0.70	0.94
0234+285	0.1393	9.51	13.47	28.59	26.73	93.91	87.65	1.14	1.51
0235+164	2.0000	36.75	53.69	31.38	29.37	102.62	96.01	0.98	1.28
0336–019	0.5788	1.64	2.40	33.40	31.07	106.40	98.71	1.87	2.54
0420–014	0.1750	10.98	16.43	19.91	18.52	128.69	118.37	0.99	1.31
0440–003	0.1825	1.71	2.44	26.89	25.03	87.61	81.54	1.45	1.92
B0454–234	0.0217	11.15	15.42	17.90	16.81	60.04	56.31	0.78	1.01
0454–463	0.0339	11.30	15.86	19.76	18.52	65.25	61.03	0.79	1.04
B0458–020	1.4240	31.48	47.20	21.93	20.53	144.35	133.07	1.39	1.84
0506–612	0.1104	9.54	13.59	28.44	26.58	92.86	86.60	1.07	1.42
B0521–365	0.0002	31.10	46.44	3.33	3.02	16.02	14.65	0.14	0.18
0528+134	18.4000	4.52	6.97	35.72	33.24	365.99	333.88	2.66	3.54
B0537–286	0.9534	6.07	8.60	25.08	23.61	193.65	183.05	2.79	3.74
0537–441	3.0100	10.46	15.96	38.05	35.41	89.91	83.95	1.48	2.00
0716+714	0.0130	2.22	3.28	58.82	55.10	52.82	50.13	1.06	1.42
0735+178	0.0130	20.03	29.37	18.36	17.12	35.55	33.48	0.53	0.70
0804+499	0.1304	12.10	17.24	70.29	66.10	82.23	77.81	1.40	1.89
0827+243	0.1827	0.67	0.95	43.63	40.84	144.07	134.26	1.97	2.61
0829+046	0.0030	12.14	18.20	6.58	6.12	36.08	33.19	0.31	0.41
0836+710	0.5480	1.67	2.53	36.65	34.17	577.54	525.40	2.15	2.82
0851+202	0.005	0.93	1.33	47.35	44.25	63.40	59.79	0.98	1.33
0906+430	0.0404	20.08	28.31	31.07	29.06	40.89	38.68	0.79	1.06
0917+449	0.5110	7.54	10.80	12.10	11.23	157.96	149.10	2.19	2.96
0954+556	0.1471	26.12	37.00	84.70	79.90	43.83	41.93	1.26	1.71
0954+658	0.0089	47.97	68.02	32.16	29.99	26.66	25.35	0.51	0.68
1011+496	0.0019	16.07	23.14	24.72	23.01	36.76	34.60	0.41	0.56
1055+567	0.0054	25.07	34.82	73.39	69.20	34.50	33.11	0.71	0.94
1101+384	0.0001	1.50	2.31	61.76	57.73	36.60	34.84	0.47	0.65
B1127–145	0.1382	5.68	7.90	33.25	31.23	63.43	61.19	1.82	2.44
1156+295	0.3485	15.85	22.64	23.39	21.86	48.27	46.29	1.66	2.28
1219+285	0.0024	2.99	4.41	7.82	7.20	28.66	26.37	0.37	0.50
1222+216	0.0246	15.23	21.80	14.02	13.09	45.37	42.27	0.57	0.76
1226+023	0.0030	8.90	13.27	13.25	12.32	60.47	56.00	0.32	0.42
B1229–021	0.0356	10.56	14.76	20.38	19.14	67.67	63.36	0.85	1.11
1253–055	1.3400	6.57	10.20	18.52	17.12	112.87	103.34	1.10	1.47
1253–055	5.7500	5.25	8.12	21.93	20.22	108.32	99.48	1.54	2.07
1331+170	0.6207	7.71	10.98	38.36	35.88	125.99	117.53	1.73	2.30
B1334–127	0.0111	17.78	24.77	37.89	35.57	44.97	42.69	0.71	0.94
B1510–089	0.0180	28.03	41.90	10.30	9.53	39.23	36.36	0.43	0.56
1604+159	0.017	17.73	25.64	10.30	9.53	32.72	30.35	0.46	0.61
1606+106	0.2595	11.75	16.57	23.17	21.77	76.37	71.43	1.16	1.52
1611+343	0.4807	16.74	23.54	88.11	83.31	75.86	72.21	1.76	2.36
1622–297	26.9000	5.44	8.51	13.40	12.47	78.69	72.10	1.69	2.28
1633+382	9.7200	3.43	5.42	32.00	29.68	321.98	292.41	2.13	2.88
1652+398	0.0003	4.01	6.27	21.31	19.76	28.19	26.53	0.30	0.40
1730–130	0.2954	11.78	16.91	27.66	25.80	89.48	83.30	1.16	1.55
1739+522	0.2713	9.36	13.32	31.23	29.21	102.07	95.23	1.31	1.74
B1741–038	0.169	7.96	11.33	42.70	39.91	140.60	131.12	1.33	1.76
1830–210	0.2561	11.34	16.02	27.51	25.65	90.37	84.32	1.18	1.56
1933–400	0.1682	11.45	16.00	25.49	23.94	84.97	79.56	1.11	1.45
2005–489	0.0002	1.98	2.80	85.40	80.44	41.18	39.52	0.63	0.86
2032+107	0.0199	10.72	15.00	22.55	21.15	75.02	70.21	0.74	0.98
2052–474	0.2603	7.64	11.07	39.91	37.12	128.67	119.54	1.42	1.90
B2155–304	0.0003	4.01	6.27	8.91	8.13	19.88	18.44	0.35	0.48
2200+420	0.0190	11.00	15.95	15.11	14.02	29.92	27.98	0.48	0.66
2230+114	0.1840	15.33	22.95	17.43	16.19	110.55	101.66	0.92	1.22
2251+158	0.3200	0.57	0.87	31.23	29.06	245.76	225.22	1.94	2.59
2356+196	0.1191	9.58	13.83	28.44	26.42	91.45	84.96	1.05	1.40

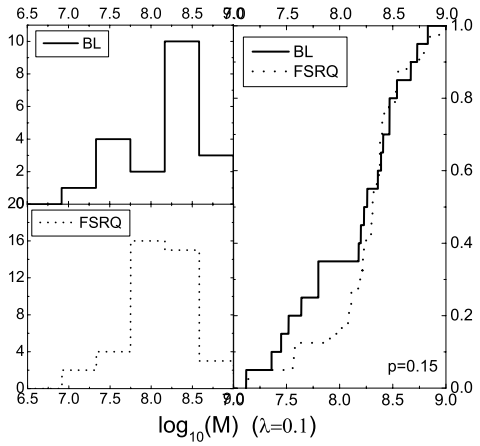

Fig. 1 Histogram of black hole mass for BLs (solid lines) and FSRQs (dotted lines) for the case of $\lambda = 0.1$.

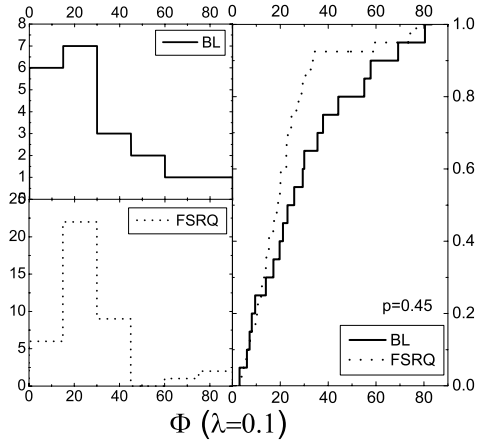

Fig. 2 Histogram of the propagation angle (Φ) for BLs (solid lines) and FSRQs (dotted lines) for the case of $\lambda = 0.1$.

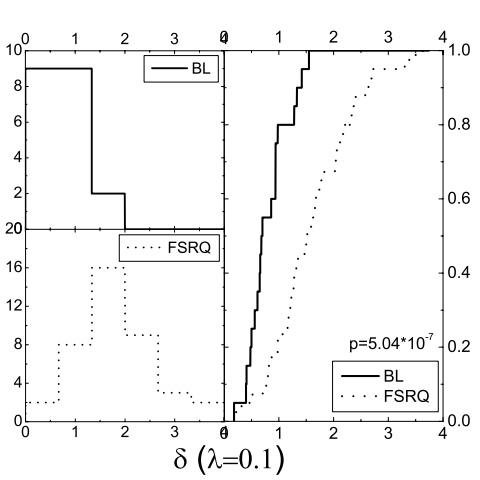

Fig. 3 Histogram of the boosting factor (δ) for BLs (solid lines) and FSRQs (dotted lines) for the case of $\lambda = 0.1$.

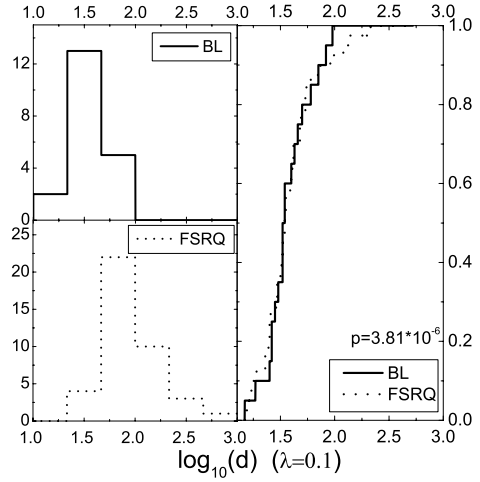

Fig. 4 Histogram of the distance of the gamma-ray emission region for BLs (solid lines) and FSRQs (dotted lines) for the case of $\lambda = 0.1$.

FSRQs separately, we have $d = (41.31 \pm 21.21)\, R_g$ for BLs and $d = (112.23 \pm 91.73)\, R_g$ for FSRQs for $\lambda = 0.1$. The probability for both to come from the same distribution is 3.81×10^{-6}, see Figure 4.

3 DISCUSSION

In AGNs, the central black hole plays an important role in observational properties and has drawn much attention. The central black hole mass perhaps sheds some light on the evolution process in AGNs

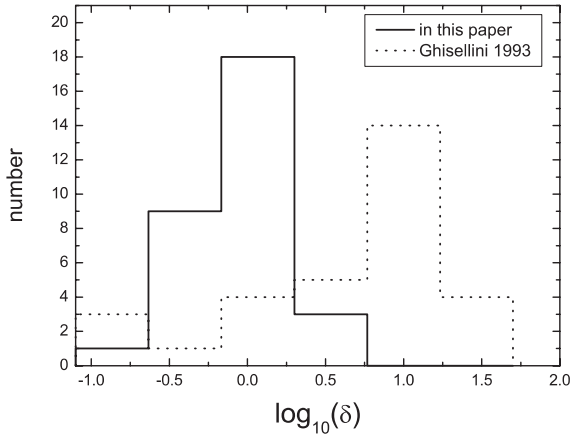

Fig. 5 Comparison between the Doppler factor estimated in the present work with those by Ghisellini et al. (1993). The solid line represents the results from this paper, and the dotted line represents those from Ghisellini et al. (1993)

(Barth et al. 2002; Cao 2002; Fan et al. 2007; Wang et al. 2006a,b; Wu 2002). There are many methods for mass determination, although the mass determination is not in consensus. In the present paper, we determined the central black hole mass for a larger sample of γ-ray loud blazars using the previous method, which is constrained by the optical depth of the $\gamma - \gamma$ pair production. As we discussed in the previous papers, this method, which is independent of the X-ray emission mechanism, can be performed for the central black hole mass determination of high redshift gamma-ray sources. We should mention that the mass determined in the present paper corresponds to the unity optical depth and therefore the results correspond to the upper limit for central black hole masses.

In the method, the X-ray emissions, the γ-ray emissions and the short time scales as well are important for the determination of the basic parameters. In our previous paper, we compiled the relevant data for 23 γ-ray loud sources (Fan 2005), while in the present paper, we obtained the relevant data for 59 γ-ray loud blazars.

BLs and FSRQs are two subclasses of blazars. From an observational point of view, except for the emission line properties (the emission line strength in FSRQs is strong while that in BLs is weak or invisible), other observational properties are quite similar between them (Fan 2003). Their relationship has drawn much attention (e.g., Sambruna et al. 1996; Scarpa & Falomo 1997; Ghisellini et al. 1998; D'Elia & Cavaliere 2000; Bottcher & Dermer 2002; Fan 2002; Ciaramella et al. 2004). Bottcher & Dermer (2002) proposed that the accretion rate rather than the central black hole masses plays an important role in the evolutionary sequence (for FSRQs evolving into BLs) of blazars. Because the accretion rate in FSRQs is much faster than that in BLs, there is not much gas in BLs to fuel the central black hole. For the 59 γ-ray loud blazars (20 BLs and 39 FSRQs), if we consider BLs and FSRQs separately, the distribution of the mass does not show much difference (see Fig. 1), and their averaged masses are $\log M/M_{\odot} = 8.07 \pm 0.41$ for FSRQs, and $\log M/M_{\odot} = 8.12 \pm 0.50$ for BLs. A K-S test indicates that the probability for the two classes to come from the same parent distribution is p = 15%. The result is consistent with that by Wu et al. (2002). That result perhaps suggests that the central black hole mass plays a less important role in the evolutionary sequence as pointed out by Bottcher & Dermer (2002).

On the average, the Doppler factors in BLs are smaller than those in FSRQs (see Fig. 5), but the propagation angles are almost the same. This property suggests that the Lorentz factors in BLs are smaller than those in FSRQs. Ghisellini et al. (1993) also found that the Doppler factors in BLs are smaller than those in FSRQs. The reason that we obtained similar angular values is that we assume the emission to be from a cone with half angle Φ while others assume that the emission is isotropic.

In this paper, the optical depth of a γ-ray traveling in the field of a two-temperature disk with a beaming effect has been used to determine the central mass, M, for 59 γ-ray loud blazars with available short timescales. The masses obtained in the present paper are in the range of $10^{7}\,M_{\odot}$ to $10^{9}\,M_{\odot}$ for the whole sample. In the case of black hole mass, there is no clear difference between BLs and FSRQs, which suggests that the central black hole masses do not play an important role in the evolutionary sequence of blazars. The Lorentz factors and Doppler factors in BLs are smaller than those in FSRQs, but they have almost the same propagation angles.

Acknowledgements This work is partially supported by the National Natural Science Foundation of China (Nos. 10573005 and 10633010) and the 973 project (No. 2007CB815405).

References

Barth, A. J., Ho, L. C., & Sargent, W. L. W. 2002, ApJ, 566, L13
Becker, P., & Kafatos, M. 1995, ApJ, 453, 83
Bednarek, W. 1993, A&A, 278, 307
Bloom, S. D., Bertsch, D. L., Hartman, R. C., et al. 1997, ApJ 490, L145 (B97)
Bottcher, M., & Dermer, C. D. 2002, ApJ, 564, 86
Cao, X. W. 2002, ApJ, 570, L13
Cheng, K. S., Fan, J. H., & Zhang, L. 1999, A&A, 352, 32
Cheng, K. S., Zhang, X., & Zhang, L. 2000, ApJ, 537, 80
Chiappetti, L., et al. 1999, ApJ, 521, 552 (Ch99)
Ciaramella, A., Bongardo, C., Aller, H. D., et al. 2004, A&A, 419, 485
Comastri, A., et al. 1997, ApJ, 480, 534 (C97)
Courvoisier, T. J.-L., Robson, E. I., Hughes, D. H., et al. 1988, Nature, 335, 330
Dermer, C. D., Schlickeiser, R., & Mastichiadis, A. 1992, A&A, 256, L27
De Jager, O. C., et al. 1999, in Proc. of 26th ICRC (Salt Lake City), 3, 346
D'Elia, V., & Cavaliere, A. 2001, ASPC, 227, 252
Dibai, E. A. 1984, SvA, 28, 245
Dondi, L., & Ghisellini, G. 1995, MNRAS, 273, 583 (D95)
Donato, D., Ghisellini, G., Tagliaferri, G., & Fossati, G. 2001, A&A, 375, 739 (D01)
Fan, J. H. 2002, PASJ, 54, L15
Fan, J. H., Xie, G. Z., & Bacon, R. 1999, A&AS, 136, 13
Fan, J. H., Adam, G., Xie, G. Z., et al. 1998, A&A, 338, 27
Fan, J. H. 2005, A&A, 436, 799
Ferrarese, L., & Merritt, D. 2000, ApJ, 539, L9
Ferrarese, L., et al. 2001, ApJ, 555, L79
Fossati, G., Maraschi, L., Celotti, A., Comastri, A., & Ghisellini, G. 1998, MNRAS, 299, 433 (F98)
Franceschini, A., Vercellone, S., & Fabian, A. C. 1998, MNRAS, 297, 817
Gebhardt, K., et al. 2000, ApJ, 543, L5
Genzel, R., et al. 1997, MNRAS, 291, 219
Ghisellini, G., Padovani, P., Celotti, A., & Maraschi, L. 1993, ApJ, 407, 65
Ghisellini, G., Celotti, A., Fossati, G., et al. 1998, MNRAS, 301, 451
Hartman, R. C., et al. 1999, ApJS, 123, 79
Hartman, R. C., Webb, J. R., Marscher, A. P., et al. 1996, ApJ, 461, 698
Hartman, R. C. 1996, in ASP Conf. Ser. 110, eds. H. R. Miller, J. R. Webb, & J. C. Noble (San Francisco: ASP), 333
Hayashida, N., Hirasawa, H., Ishikawa, F., et al. 1998, ApJ, 504, L71
Ho, L. C. 2002, ApJ, 564, 120
Kaspi, S., Smith, P. S., Netzer, H., Maoz, D., Jannuzi, B. T., & Giveon, U. 2000, ApJ, 533, 631
Kataoka, J., Mattox, J. R., Quinn, J., et al. 1999, APh, 11, 149
Kniffen, D. A., Bertsch, D. L., Fichtel, C. E., et al. 1993, ApJ, 411, 133 (K93)
Komossa, S., Burwitz, V., Hasinger, G., et al. 2003, ApJ, 582, L15

Kormendy, J., & Richstone, D. 1995, ARA&A, 33, 581
Kormendy, J., & Gehbardt, K. 2001, in AIP Conf. Ser. 586, 20th Texas Symposium on Relativistic Astrophysics, eds. H. Martel, & J. C. Wheeler (New York: AIP), 363
Kranich, D., Mirzoyan, R., Petry, D., et al. 1999, APh, 12, 65
Laor, A. 1998, ApJ, 505, L83
Lawson, A. J., & McHardy, I. M. 1998, MNRAS, 300, 1023
Madejski, G., et al. 1996, ApJ, 459, 156
Magorrian, J., et al. 1998, AJ, 115, 2285
Mattox, J. R., Bertsch, D. L., Chiang, J., et al. 1993, ApJ, 410, 609 (M93)
Mattox, J. R., Wagner, S. J., Malkan, M., et al. 1997, ApJ, 476, 692 (M97)
McLure, R. J., & Dunlop, J. S. 2001, MNRAS, 327, 199
Miller, H. R. 1978, PASP, 90, 661
Merritt, D., & Ferrarese, L. 2001, in ASP Conf. Proc. 249, The Central Kiloparsec of Starbursts and AGNs, eds. J. H. Knapen, J. E. Beckman, et al. (San Francisco: ASP), 335
Padovani, P., & Rafanelli, P. 1988, A&A, 205, 53
Perlman, E. S., et al. 1996, ApJS, 104, 251
Pica, A. J., et al. 1988, AJ, 96, 1215 (P88)
Quinn, J., Akerlof, C. W., Biller, S., et al. 1996, ApJ, 456, L83 (Q96)
Rieger, F. M., & Mannheim, K. 2000, A&A, 359, 948
Rieger, F. M., & Mannheim, K. 2003, A&A, 397, 121
Sambruna, R. M., Maraschi, L., & Urry, C. M. 1996, ApJ, 463, 444
Scarpa, R., & Falomo, R. 1997, A&A, 325, 109
Sillanpaa, A., Haarala, S., Valtonen, M. J., et al. 1988, ApJ, 325, 628
Stacy, J. C., Vestrand, W. T., Sreekumar, P., et al. 1996, A&AS, 120, 549
Urry, C. M., et al. 1997, ApJ, 486, 799
Vestergaard, M. 2002, ApJ, 571, 733
Villata, M., & Raiteri, C. M. 1999, A&A, 347, 30
Von Montigny, C., Bertsch, D. L., Chiang, J., et al. 1995, ApJ, 440, 525
Wandel, A., & Yahil, A. 1985, ApJ, 295, L1
Wandel, A., Peterson, B. M., & Malkan, M. A. 1999, ApJ, 526, 579
Wang, J. M., et al. 2006a, ApJ, 642, L111
Wang, J. M., et al. 2006b, ApJ, 647, L17
Wehrle, A. E., Pian, E., Urry, C. M., et al. 1998, ApJ, 497, 178 (W98)
Wills, B. J. 1971, ApJ, 169, 221
Wu, X. B., Liu, F. K., & Zhang, T. Z. 2002, A&A, 389, 742
Xie, G. Z., Liu, F. K., & Liu, B. F. 1991, A&A, 249, 65
Xie, G. Z., Zhou, S. B., & Liang, E. W. 2004, ApJ, 127, 53 (X04)
Xie, G. Z., Zhou, S. B., Dai, B. Z., Liang, E. W., et al. 2002, MNRAS, 329, 689
Zhang, L., & Cheng, K. S. 1997, ApJ, 475, 534